RSC Advances

ROYAL SOCIETY OF CHEMISTRY

www.rsc.org/advances

Polarizability Series of Aqueous Polyatomic Anions Revealed by Femtosecond Kerr Effect Spectroscopy

Mengqi Hou, Rong Lu* and Anchi Yu*

Department of Chemistry, Renmin University of China, Beijing 100872, P. R. China

Submitted for publication in *RSC Advances*

*Corresponding authors

Email: lvrong@chem.ruc.edu.cn

Phone: +86-10-6251-5043

Fax: +86-10-6251-6444

Email: a.yu@chem.ruc.edu.cn

Phone: +86-10-6251-4601

Fax: +86-10-6251-6444

Abstract:

The polarizability or hyperpolarizability of aqueous anion is closely related to the important processes such as surface tension change of water and the empirical Hofmeister Effect. Herein, we measured the hyperpolarizabilities of six polyatomic anions (HPO_4^{2-}, HSO_4^-, CO_3^{2-}, CH_3COO^-, NO_3^- and SCN^-) in their aqueous potassium salt solutions by using femtosecond optical Kerr effect spectroscopy. We found that the hyperpolarizability of those six aqueous anions present the increasing series as the following rank: $HPO_4^{2-} \sim HSO_4^- < CO_3^{2-} < CH_3COO^- < NO_3^- < SCN^-$, which is correlated well with the Hofmeister series of aqueous anions as a decreasing ability to precipitate protein. But CO_3^{2-} anion is the exceptional anion. The current study is useful for disclosing the fundamental physicochemical phenomenon in aqueous salt solutions.

Keywords: Hyperpolarizability, Anion, Hofmeister Series, Aqueous Potassium Salt Solution, Femtosecond Optical Heterodyne-Detected Raman Induced Kerr Effect Spectroscopy

1. Introduction

The presence of ions in water can cause some vital important phenomena such as the surface tension change of water and the empirical Hofmeister series.[1-4] However, the physical mechanisms of the ion effects on those phenomena are not yet completely understood.[5] In the recent, Rogers *et al.* utilized quasichemical theory to analyze the effects of the anion's polarization and size on the Hofmeister series of Cl^-, Br^- and I^- anions, and they found that the polarizability of the anion has more obvious effect on the local solvation structure around the anion than its size does.[6] Using molecular dynamics simulations, Vrbka *et al.* found that the polarizability of the anion is a key determinant of the surface specificity, and they pointed out that the hard and non-polarizable ions are repelled from the interface, while the soft and polarizable ions exhibit surface affinity.[7] These studies indicate that the polarizability of the anion plays a crucial role in most aqueous salt systems. The polarizabilities of many anions have been theoretically calculated in aqueous solutions.[6, 8-13] However, there exist only several experimental reports to study the polarizabilities of anions.[14, 15] Therefore, more experimental studies on the measurement of the polarizability or hyperpolarizability of the anion in aqueous solutions are in great need.

Femtosecond Kerr effect spectroscopy is able to provide the ultrafast nuclear dynamics of transparent media and its fast Fourier transform (FFT) spectrum would offer the Raman spectral density in the low frequency range from 1 to 400 cm^{-1}.[16, 17] The origin of the optical Kerr effect includes both the electronic and nuclear hyperpolarizability in molecular liquids.[17, 18] The nuclear contributions further include the anisotropic polarizability, intermolecular interaction induced polarizability change, and nuclear-coordinate-dependent polarizability change.[17, 18] Because the electronic contribution doesn't reflect the molecular motions and the nuclear-coordinate-dependent polarizability change is associated with intramolecular vibration, these two parts are not considered generally. In the studies of ultrafast Kerr effect spectroscopy, the most frequently used technique is Femtosecond Optical Heterodyne-Detected Raman Induced Kerr Effect Spectroscopy (fs OHD-RIKES), which have been widely applied to explore the soft condensed systems in time or frequency domain.[16] The fs OHD-RIKES signal is

sensitive to polarizability anisotropy so that a group with a high-symmetry structure makes less contribution to the anisotropic fs OHD-RIKES measurement.[17]

Femtosecond OHD-RIKES has been employed to investigate the relaxation dynamics and the intermolecular hydrogen bonding in pure water,[19, 20] aqueous alkali halide solution,[21, 22] and aqueous sodium nitrate solution.[23] However in literatures, there are no systematical studies on the anion's hyperpolarizability in aqueous solution with fs OHD-RIKES measurement. In this work, we selected six polyatomic anions (HPO_4^{2-}, HSO_4^-, CO_3^{2-}, CH_3COO^-, NO_3^- and SCN^-) and measured their respective hyperpolarizability in the potassium salt aqueous solutions by using fs OHD-RIKES. All selected anions are related to the anionic Hofmeister series: $CO_3^{2-} > SO_4^{2-} > F^- > HPO_4^{2-} > CH_3COO^-$ (AC^-) $> Cl^- > Br^- > NO_3^- > I^- > ClO_4^- > SCN^-$,[4, 24] where the SCN^- is the most effective denaturant of proteins.[25] Besides, the HPO_4^{2-} anion is one of the main forms in phosphate buffer solution which is one of the major pH controlling systems in protein science and human body. Taking the value of the hyperpolarizability of H_2O as the standard,[12] we obtained the hyperpolarizabilities of all selected anions in aqueous solutions.

2. Experimental Section

Ultrapure H_2O (18.2 MΩ • cm) was obtained through a Milli-Q water purification system (Millipore, USA). Potassium thiocyanate (KSCN, > 99.8%) and Potassium phosphate dibasic (K_2HPO_4, > 99.8%) were purchased from J&K Chemical LTD. Potassium Carbonate (K_2CO_3, > 99.997%) was purchased from Alfa Aesar. Potassium acetate (KAC, > 99%) was purchased from Acros organics. Potassium bisulfate ($KHSO_4$, > 99.995%) was purchased from Fluka. Potassium nitrate（KNO_3, > 99.999%）was purchased from Strem chemicals Newburyport, MA, USA.

The fs OHD-RIKES measurement are described in detail elsewhere.[26] Briefly, pulses with 80 MHz from a femtosecond Ti: Sapphire laser were sent through a prism compressor and split into two beams: one for the pump and one for the probe. Both the pump and the probe pulses were firstly vertical polarized by two Glan-Taylor polarizers, and then the polarization of the pump pulses was tuned to 45 degree with respective to the probe pulses polarization through a λ/2 waveplate to achieve the most

efficient Optical Kerr signal. Another Glan-Taylor polarizer was placed in the probe beam after the sample and set to be perpendicular to the Glan-Taylor polarizer in the probe beam before the sample. In order to achieve the heterodyne detection, a λ/4 waveplate was placed in the probe beam between the sample and the Glan-Taylor polarizer before the sample, and the λ/4 waveplate was set at 1 degree away from its fast optical axis to introduce a local field. The femtosecond OHD-RIKES signal was collected by a fast time response photodiode and sent to a lock-in amplifier where it was synchronized by an optical chopper. The chopped frequency was 2.0 kHz. The laser pulse spectra centered at 800 nm with an 18 nm full width at half maximum. The pulses had 55 fs time duration. The pump and probe pulse powers at the sample's position were about 70 mW and 15 mW, respectively. 10 scans for each sample with 1 μm/step resolution were recorded in the time range from -0.5 to 7.5 picoseconds.

A 3-mm path length fused silica cell was used in the fs OHD-RIKES measurements and all aqueous solutions were filtered by 0.2 micro-filters to remove the scattering particles before each optical measurement.

3. Results and Discussion

Figure 1 shows the normalized fs OHD-RIKES signals of 4.0 M K_2HPO_4, 4.0 M K_2CO_3, 4.0 M KAC, 4.0 M KSCN, 3.1 M KNO_3 and 3.5 M $KHSO_4$ aqueous solutions within 7.5 picoseconds. The fs OHD-RIKES signal of pure water is also plotted in Figure 1 as a reference. The sharp peak at around zero time is the instantaneous electronic response. The intermediate and more slowly processes arise from the nuclear motions. From the data shown in Figure 1, it is obvious that the nuclear contributions arising from SCN^-, NO_3^-, AC^- and CO_3^{2-} anions are larger than the nuclear contributions from HSO_4^- and HPO_4^{2-} anions, which are comparable to that of pure water.

To compare the relative magnitudes of the hyperpolarizability of the corresponding anion, we convert their respective fs OHD-RIKES signals from time domain to frequency domain with the regular data analysis procedure.[27] Briefly, we first removed the rotational contribution from the original fs OHD-RIKES time domain data through subtracting a single exponential decay fit in the time range of 0.5 –

7.5 ps. Then, we performed the fast Fourier transform (FFT) operation on the residue fs OHD-RIKES signal and the laser pulse autocorrelation response, respectively. Finally, we took the imaginary part of the complex division of the FFT of the residue fs OHD-RIKES signal by the FFT of the laser pulse autocorrelation response as the fs OHD-RIKES FFT spectrum. During this procedure, we carefully check the zero time delay effect on the fs OHD-RIKES FFT spectrum. A criterion for determining the suitable time delay between autocorrelation curve and fs OHD-RIKES maximal signal was to make the base line of the fs OHD-RIKES FFT spectrum flat and close to zero above 400 cm^{-1}. Figure 2 shows the low frequency fs OHD-RIKES FFT spectra of all selected six anions potassium salt solutions and pure water.

The low frequency fs OHD-RIKES FFT spectra and low frequency Raman spectra of pure water or aqueous salt solutions often have two intermolecular vibrational bands: one band locates at around 50 cm^{-1} which is assigned to the translational or bending motion of the intermolecular hydrogen bond of water, and another band locates at around 180 cm^{-1} which is assigned to the longitudinal or stretching motion of the intermolecular hydrogen bond of water.[19-21, 28-30] However, previous experimental and theoretical studies on salt solutions revealed that the mode associated with the 180 cm^{-1} band are related to the connectivity of the hydrogen bonding network, and that the 50 cm^{-1} band is independent of the existence of hydrogen bonds.[31-33] Our earlier result also suggested that the 50 cm^{-1} band in the low frequency fs OHD-RIKES FFT spectrum of high concentrated aqueous salt solution is related to the collective motion of its anion.[26] Therefore, we assigned the around 50 cm^{-1} band in the fs OHD-RIKES FFT spectrum shown in Figure 2 is the contribution of respective aqueous anion.

The fs OHD-RIKES mainly measure the sample's electronic and nuclear hyperpolarizability, thus the amplitude intensity of the 50 cm^{-1} band reflects the nuclear hyperpolarizability of respective anion in aqueous solutions. From the data shown in Figure 2, it is found that the magnitudes of all selected anion's hyperpolarizabilities in aqueous solutions is in the decreasing sequence as $SCN^- > NO_3^- > AC^- > CO_3^{2-} > HSO_4^- \sim HPO_4^{2-}$. Parson *et al* calculated the static polarizabilities of all those six anions and found that the static polarizabilities of all those six anions is in the decreasing sequence as SCN^- >

CO_3^{2-} > $HPO4^{2-}$ > AC^- > HSO_4^- > NO_3^-.[12] The difference in the sequence revealed by the static polarizabilities and the hyperpolarizability measurements is due to the contribution of the interaction induced polarizability. Mason *et al.* performed polarizable simulation on NO_3^- and CO_3^{2-}, respectively, and found that the polarizability of NO_3^- is higher than that of CO_3^{2-} in aqueous solution,[34] which is in agreement with our current measurement. Spange *et al.* used solvatochromic method to explore the polarizabilities of 1-alkyl-3-methylimidazolium ionic liquids with different anions and found that the polarizability of SCN^- is larger than that of NO_3^-,[14] which is also accord with our results. Howard *et al.* calculated the polarizabilities of ClO_4^-, HSO_4^- and $H_2PO_4^-$ anions respectively, and found that their mean molecular polarizabilities differ very little among them,[35] which is also in accord with our current findings on the situation of HSO_4^- and HPO_4^{2-}. Unfortunately, due to the low solubility of potassium perchlorate in aqueous solution, we cannot investigate ClO_4^- in the current study.

To further investigate the hyperpolarizabilities of those anions in aqueous solutions, we recorded the fs OHD-RIKES signals of all selected six salts at different concentrations, as shown in Figure 3. Clearly, the intensity of the fs OHD-RIKES signals of the SCN^-, NO_3^-, AC^-, CO_3^2 and HSO_4^- anions after 100 fs increases with the increase of the salt concentration. However, the concentration dependent fs OHD-RIKES signal of HPO_4^{2-} anion presents a reverse trend as the other anion solutions. Besides, the intensity of the fs OHD-RIKES signals of HSO_4^- anion does not increase much from 0.2 M to 3.5 M. Mazur *et al.* studied the trimethylamine N-oxide (TMAO) aqueous solution and found a similar phenomenon with our study. They suggested that the water structure is preserved in the TMAO solution even at 4 M concentration.[36] Tobias *et al.* calculated the polarizability of sulfate dianion in the aqueous bulk and found that sulfate dianion remain almost isotropic.[11] Therefore, we suggested that HSO_4^- also keep nearly spherical symmetry structure in aqueous solution and its tetrahedral structure is rigid. As a consequence, the intrinsic anisotropic polarizability and the interaction induced polarizability of HSO_4^- anion are negligible in our fs OHD-RIKES measurements.

To quantitatively explore the hyperpolarizability of the selected anions in aqueous solutions, we took the value of their OHD-RIKES signal at 250 fs position (Figure 3) and obtained the concentration

dependent fs OHD-RIKES intensity of all selected salt solutions, as shown in Figure 4. The reason that we selected the OHD-RIKES value at 250 fs position is to eliminate the interference of the electronic hyperpolarizability. With the linear region data shown in Figure 4, we obtained the slopes for the concentration dependent intensity of the fs OHD-RIKES signal of all selected salt solutions, as listed in Table 1. Maroulis calculated the hyperpolarizability of H_2O and found that its value is 6.104×10^{-62} $C^4\cdot m^4\cdot J^{-3}$.[37] Taking the hyperpolarizability value of H_2O as the standard, we obtained the hyperpolarizability of all selected anions in aqueous solutions, which are listed in Table 1. Although Maroulis has argued that the value of the hyperpolarizabililty of H_2O is dependent on the selected basis set and it has some difference with the electric induced optical second harmonic generation's result,[37] it is still reasonable to be used as a reference value in our current study. From the data listed in Table 1, it is obvious that the obtained hyperpolarizabilities of anions also present the decreasing sequence in the order of $SCN^- > NO_3^- > AC^- > CO_3^{2-} > HSO_4^- \sim HPO_4^{2-}$. The nonlinear increase of the fs OHD-RIKES value at 250 fs position under high salt concentration indicates that the ion pairs could present and has a certain of effect on the fs OHD-RIKES spectra shown in Figure 2. However, the effect of the ion pairs on the fs OHD-RIKES spectra at high electrolyte solutions is beyond the intent of our current study.

The HPO_4^{2-} is one of the main forms in phosphate buffer solution which is one of the major pH controlling systems in protein science. From the data shown in Figure 3 and Figure 4, we found that the intensity of the fs OHD-RIKES signals of HPO_4^{2-} anion presents the decreasing trend along with the increasing of the salt concentration. In Figure 5, we displayed the low frequency fs OHD-RIKES FFT spectra of 0.2 M and 4.0 M K_2HPO_4 solutions together with pure water, which both are normalized at 50 cm^{-1}. Obviously, the intensity of 180 cm^{-1} band in the low frequency spectra of 0.2 M K_2HPO_4 solution is smaller than that of pure water. The intensity of 180 cm^{-1} band in the low frequency spectra of 4.0 M K_2HPO_4 solution is larger than that of pure water. It has demonstrated that the 180 cm^{-1} band are associated with the connective hydrogen bonding of water. Therefore, we concluded that the appearance of the larger 180 cm^{-1} band in the low frequency spectra of 4.0 M K_2HPO_4 solution is due to the strong hydrogen bonding of water. Ahmed *et al.* used Raman spectroscopy in combination with

multivariate curve resolution to explore Na-salt solutions, and they suggested that strong hydrogen bonding of water exists in the hydration shell of PO_4^{3-} anion,[38] which is consistent with our fs OHD-RIKES measurement of HPO_4^{2-}.

Herein, we achieved the increasing hyperpolarizability series of aqueous anions as the following rank: HSO_4^- < HPO_4^{2-} < CO_3^{2-} < AC^- < NO_3^- < SCN^- with fs OHD-RIKES measurement. Comparing with the empirical anion's Hofmeister series: CO_3^{2-} > SO_4^{2-} > F^- > HPO_4^{2-} > AC^- > Cl^- > Br^- > NO_3^- > I^- > ClO_4^- > SCN^-, we found that the increasing hyperpolarizability series of aqueous anions are related to the decreasing ability anionic Hofmeister series to precipitate the protein. But CO_3^{2-} anion is the most exceptional anion when comparing the two series. The reversal of the Hofmeister series happens when various related phenomenon are used to define this series, such as for anions $H_2PO_4^-$, SO_4^{2-}, ClO_4^- and SCN^-,[5] but we have not yet find the reversal of CO_3^{2-} anion derived from our hyperpolarizability measurement. Most importantly, we obtained the hyperpolarizabilities of all selected anions in aqueous solutions with the hyperpolarizability value of H_2O as a reference. The current study suggests that the hyperpolarizability of aqueous anion may be one of the key factors determining the Hofmeister series, which confirms the recent theoretical findings.[6]

4. Conclusion

In summary, the hyperpolarizabilities of six aqueous polyatomic anions (HSO_4^-, HPO_4^{2-}, CO_3^{2-}, CH_3COO^-, NO_3^- and SCN^-) in their aqueous potassium salt solutions were measured by fs OHD-RIKES technique. It is found that the hyperpolarizability of those six aqueous anions presents as an increasing rank: HPO_4^{2-} < HSO_4^- < CO_3^{2-} < AC^- < NO_3^- < SCN^-. When comparing with the empirical Hofmeister series, except for the CO_3^{2-} anion, the hyperpolarizability series of those six aqueous anions is correlated well with the anion's Hofmeister series, which suggests that the hyperpolarizability of aqueous anion may be one of the key factors determining the Hofmeister series. In addition, the 180 cm^{-1} band of the low frequency spectrum of aqueous HPO_4^{2-} become stronger at 4.0 M than that at 0.2 M, and even become stronger than the 180 cm^{-1} band of the low frequency spectrum of pure water, which suggested HPO_4^{2-} anion having an ability to promote the hydrogen bond network in aqueous solution.

Acknowledgements This work was supported by the National Natural Science Foundation of China (21273280) and by the Fundamental Research Funds for the Central Universities and the Research Funds of Renmin University of China (10XNJ047).

References

1. W. Kunz, J. Henle, and B. W. Ninham, *Curr. Opin. Colloid Interface Sci.*, 2004, **9**, 19-37.
2. Y. Levin, *Phys. Rev. Lett.*, 2009, **102**, 147803.
3. P. Jungwirth and D. J. Tobias, *Chem. Rev.*, 2006, **106**, 1259-1281.
4. P. Lo Nostro and B. W. Ninham, *Chem. Rev.*, 2012, **112**, 2286-2322.
5. Y. Marcus, *Chem. Rev.*, 2009, **109**, 1346-1370.
6. D. M. Rogers and T. L. Beck, *J. Chem. Phys.*, 2010, **132**, 014505.
7. L. Vrbka, M. Mucha, B. Minofar, P. Jungwirth, E. C. Brown, and D. J. Tobias, *Curr. Opin. Colloid Interface Sci.*, 2004, **9**, 67-73.
8. J. J. Molina, S. Lectez, S. Tazi, M. Salanne, J. F. Dufreche, J. Roques, E. Simoni, P. A. Madden, and P. Turq, *J. Chem. Phys.*, 2011, **134**, 014511
9. P. Jungwirth and D. J. Tobias, *J. Phys. Chem. A*, 2002, **106**, 379-383.
10. P. Salvador, J. E. Curtis, D. J. Tobias, and P. Jungwirth, *Phys. Chem. Chem. Phys.*, 2003, **5**, 3752-3757.
11. P. Jungwirth, J. E. Curtis, and D. J. Tobias, *Chem. Phys. Lett.*, 2003, **367**, 704-710.
12. D. F. Parsons and B. W. Ninham, *J. Phys. Chem. A*, 2009, **113**, 1141-1150.
13. D. F. Parsons and B. W. Ninham, *Langmuir*, 2010, **26**, 1816-1823.
14. R. Lungwitz, V. Strehmel, and S. Spange, *New J. Chem.*, 2010, **34**, 1135-1140.
15. K. Bica, M. Deetlefs, C. Schroder, and K. R. Seddon, *Phys. Chem. Chem. Phys.*, 2013, **15**, 2703-2711.
16. N. A. Smith and S. R. Meech, *Int. Rev. Phys. Chem.*, 2002, **21**, 75-100.
17. D. McMorrow, W. T. Lotshaw, and G. A. Kenney-Wallace, *IEEE J. Quantum Electron.*, 1988, **24**, 443-454.
18. T. Hattori and T. Kobayashi, *J. Chem. Phys.*, 1991, **94**, 3332-3346.
19. S. Palese, L. Schilling, R. J. D. Miller, P. R. Staver, and W. T. Lotshaw, *J. Phys. Chem.*, 1994, **98**, 6308-6316.
20. E. W. Castner, Y. J. Chang, Y. C. Chu, and G. E. Walrafen, *J. Chem. Phys.*, 1995, **102**, 653-659.
21. I. A. Heisler, K. Mazur, and S. R. Meech, *J. Phys. Chem. B*, 2011, **115**, 1863-1873.
22. I. A. Heisler and S. R. Meech, *Science*, 2010, **327**, 857-860.
23. I. Santa, P. Foggi, R. Righini, and J. H. Williams, *J. Phys. Chem.*, 1994, **98**, 7692-7701.

24. D. J. Tobias and J. C. Hemminger, *Science*, 2008, **319**, 1197-1198.
25. P. E. Mason, G. W. Neilson, C. E. Dempsey, A. C. Barnes, and J. M. Cruickshank, *Proc. Natl. Acad. Sci. U. S. A.*, 2003, **100**, 4557-4561.
26. R. Lu, W. Wang, Q. F. Sun, and A. C. Yu, *Chem. Phys.*, 2012, **407**, 46-52.
27. D. McMorrow, *Opt. Commun.*, 1991, **86**, 236-244.
28. G. E. Walrafen, *J. Chem. Phys.*, 1964, **40**, 3249-3256.
29. T. Ujike, Y. Tominaga, and K. Mizoguchi, *J. Chem. Phys.*, 1999, **110**, 1558-1568.
30. Y. Wang and Y. Tominaga, *J. Chem. Phys.*, 1994, **101**, 3453-3458.
31. J. Marti, J. A. Padro, and E. Guardia, *J. Chem. Phys.*, 1996, **105**, 639-649.
32. T. Nakayama, *Phys. Rev. Lett.*, 1998, **80**, 1244-1247.
33. J. A. Padro and J. Marti, *J. Chem. Phys.*, 2003, **118**, 452-453.
34. P. E. Mason, E. Wernersson, and P. Jungwirth, *J. Phys. Chem. B*, 2012, **116**, 8145-8153.
35. S. T. Howard, G. A. Attard, and H. F. Lieberman, *Chem. Phys. Lett.*, 1995, **238**, 180-186.
36. K. Mazur, I. A. Heisler, and S. R. Meech, *J. Phys. Chem. B*, 2011, **115**, 2563-2573.
37. G. Maroilis, *J. Chem. Phys.*, 1991, **94**, 1182.
38. M. Ahmed, V. Namboodiri, A. K. Singh, J. A. Mondal, and S. K. Sarkar, *J. Phys. Chem. B*, 2013, **117**, 16479-16485.

Figure Captions

Figure 1 Normalized fs OHD-RIKES signals of 4.0 M K_2HPO_4, 4.0 M K_2CO_3, 4.0 M KAC, 4.0 M KSCN, 3.1 M KNO_3 and 3.5 M $KHSO_4$ solutions within 7.5 picoseconds. The fs OHD-RIKES signal of water is plotted in black as a reference. The saturated concentrations of KNO_3 and $KHSO_4$ at room temperature are about 3.2 and 3.6 M, respectively.

Figure 2 Low frequency fs OHD-RIKES FFT spectra of 4.0 M K_2HPO_4, 4.0 M K_2CO_3, 4.0 M KAC, 4.0 M KSCN, 3.1 M KNO_3 and 3.5 M $KHSO_4$ solutions within 400 cm^{-1}. The fs OHD-RIKES signal of water is plotted in black as a reference. The saturated concentrations of KNO_3 and $KHSO_4$ at room temperature are about 3.2 and 3.6 M, respectively.

Figure 3 Concentration dependent fs OHD-RIKES signals of K_2HPO_4, K_2CO_3, KAC, KSCN, KNO_3, $KHSO_4$ aqueous solutions within 2.0 picoseconds. The fs OHD-RIKES signal of water is plotted in black as a reference.

Figure 4 Concentration dependence of the fs OHD-RIKES intensity at 250 fs position for K_2HPO_4, K_2CO_3, KAC, KSCN, KNO_3, $KHSO_4$ aqueous solutions.

Figure 5 Low frequency fs OHD-RIKES FFT spectra of 0.2 M K_2HPO_4 and 4.0 M K_2HPO_4 solutions, normalized at 50 cm^{-1} position. The fs OHD-RIKES signal of water is plotted in black as a reference.

Table 1. Summary of the polarizability α, dipolarity π^* and hyperpolarizability γ for different anions.

anions	Slope / M^{-1}	γ_{anion} [a] / 10^{-60} C^4 m^4 J^{-3}	α_0 [b] / Å^3	α_x [b] / Å^3	α_y [b] / Å^3	α_z [b] / Å^3	π^* [c]
SCN^-	0.09963	14.78	7.428	6.154	6.153	9.977	1.06
NO_3^-	0.04796	7.11	4.008	4.618	4.618	2.787	1.04
AC^-	0.01535	2.27	5.607	6.157	6.169	4.496	
CO_3^{2-}	0.00793	1.17	6.043	6.601	6.601	4.928	
HSO_4^-	0.00072	0.11	5.089	5.162	5.086	5.019	
HPO_4^{2-}	-0.00170	-0.25	6.846	6.994	6.811	63732	

[a] γ_{anion}=(Slope/0.02283) ×55.5×γ_{H2O} , γ_{H2O} is taken from reference 36 and the value is 6.104×10^{-62} C^4 m^4 J^{-3}. [b] α_0: static polarizabilities; α_x, α_y and α_z are static anisotropic polarizabilities, values of those parameters are taken from reference 12. [c] π^* are taken from reference 33.

Figures

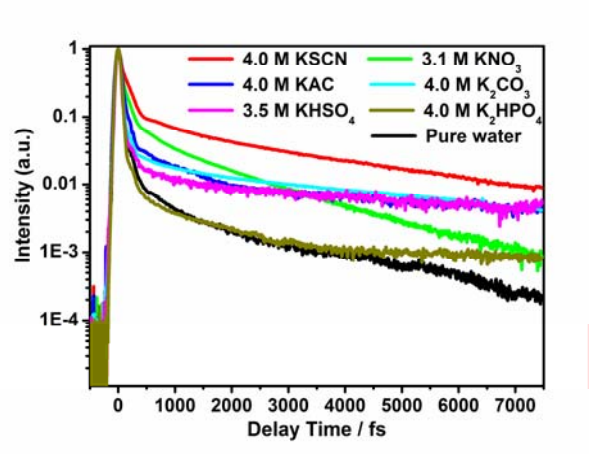

Figure 1

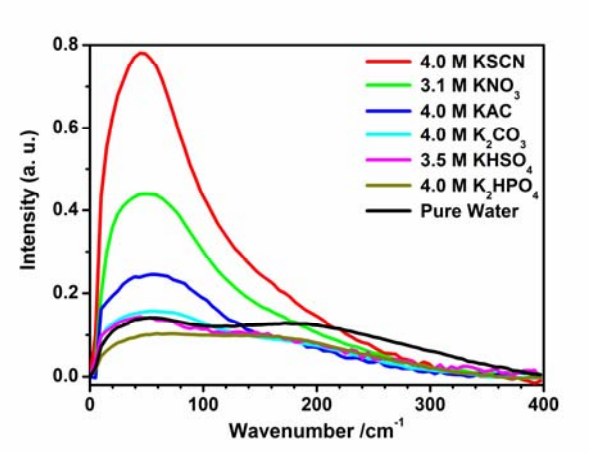

Figure 2

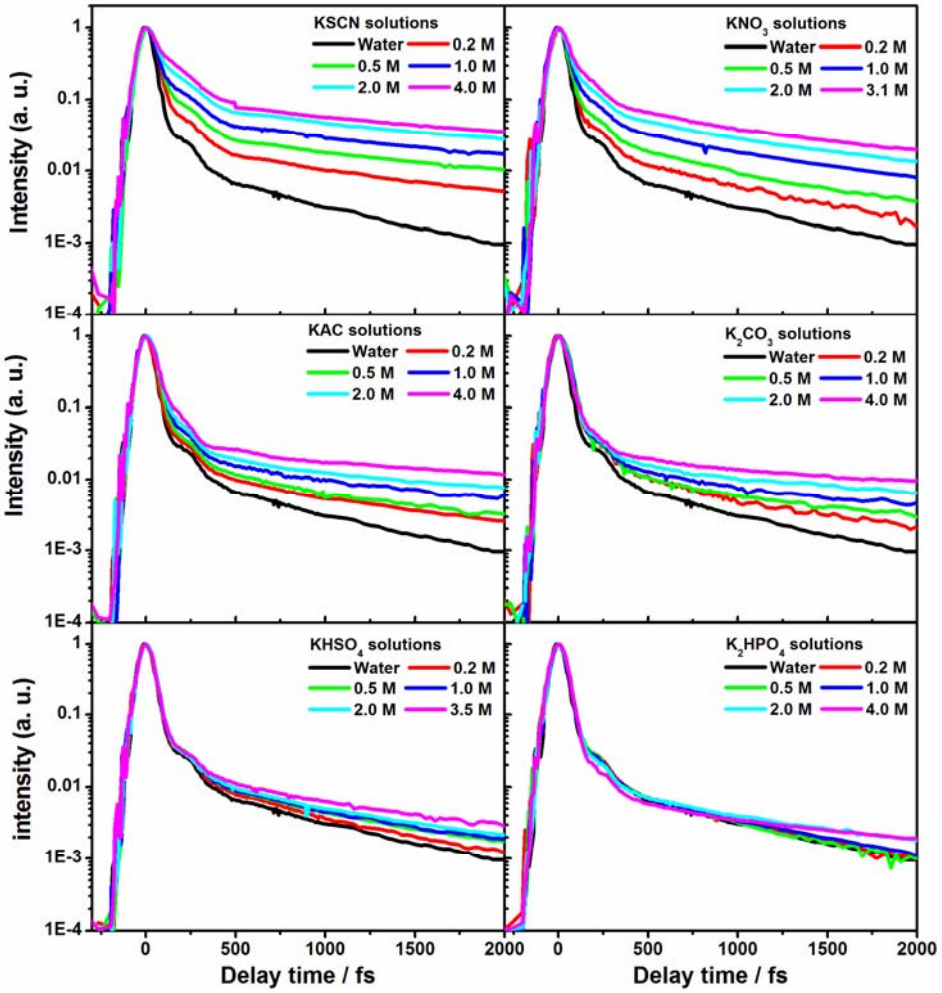

Figure 3

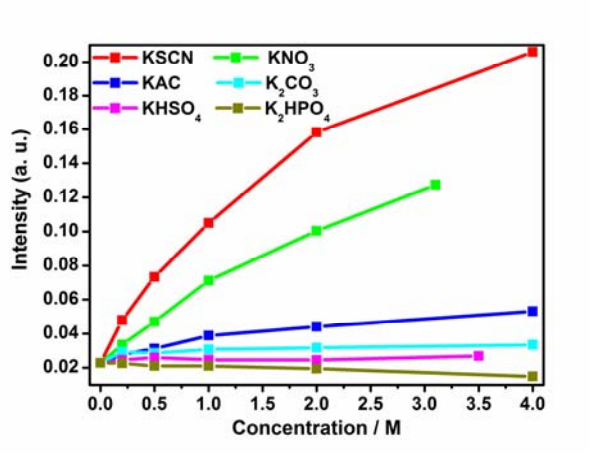

Figure 4

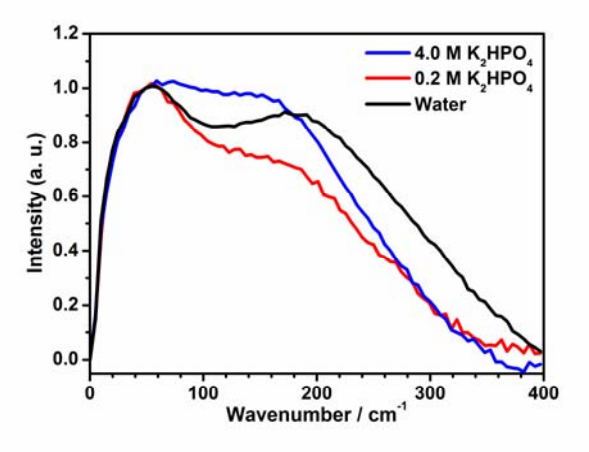

Figure 5

TOC Figure

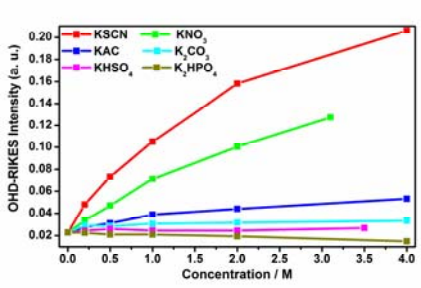

TOC Figure Caption:

The femtosecond OHD-RIKES measurements show that the hyperpolarizability series of aqueous polyatomic anions follow the increasing sequence as $HPO_4^{2-} < HSO_4^- < CO_3^{2-} < AC^- < NO_3^- < SCN^-$.